ORIGINAL RESEARCH

Proton Spectroscopy and Imaging at 3T in Ataxia-Telangiectasia

L.I. Wallis
P.D. Griffiths
S.J. Ritchie
C.A.J. Romanowski
G. Darwent
I.D. Wilkinson

BACKGROUND AND PURPOSE: Ataxia-telangiectasia (A-T) is an autosomal recessive disorder with characteristic neurodegeneration of the cerebellum. We used MR spectroscopy to test the hypothesis that cerebellar metabolism in A-T patients would be abnormal relative to healthy controls.

METHODS: Twelve adults with A-T and 12 healthy control subjects underwent MR imaging and long-echo time ^{1}H-MR spectroscopy at 3T. Voxels were acquired in the region of the dentate nucleus of the cerebellum and in parietooccipital white matter, and ratios for *N*-acetylaspartate (NAA), choline (Cho), and creatine (Cr) were calculated.

RESULTS: All of the A-T patients showed marked cerebellar atrophy of the vermis and hemispheres. Two patients showed multiple small foci of hypointensity on T2*-weighted images throughout their brain suggestive of capillary telangiectasia. A further 2 patients had single low-signal-intensity foci. One patient had a tumor, thought to be meningioma radiologically, that was not suspected clinically. No group differences were found in the cerebral spectra, but analysis of the cerebellum revealed significantly lower NAA/Cho and higher Cho/Cr ratios in the A-T patients compared with the controls. There was no difference between groups for the NAA/Cr ratio.

CONCLUSION: The findings suggest increased Cho signal intensity in the cerebellum of adult A-T patients. If this finding is shown through the course of the disease, it may assist in the differentiation of early A-T from other forms of ataxia and provide a marker for monitoring treatment efficacy.

Ataxia-telangiectasia (A-T) is an autosomal recessive multisystem disorder caused by a defective gene localized to chromosome 11q22–23 and cloned in 1995.[1-3] The estimated frequency of A-T is in the range of 1 per 40,000 to 300,000 live births.[4] A-T is an early-onset progressive neurologic disorder with a complex phenotype. Cerebellar ataxia is the clinical hallmark of the disease, present in all cases, which usually becomes apparent between 2 and 4 years of age, after a child begins to walk.[5] The ataxia is progressive and most patients are wheelchair-bound by adolescence.[6] Other clinical manifestations include somatic telangiectasia (dilated blood vessels) on the conjunctivae and skin, immunodeficiency causing a predisposition to sinopulmonary infection, elevated α-fetoprotein, and hypogonadism.[7-10]

A-T patients also have a predisposition to malignancies, of which the predominant types are lymphomas and lymphoid leukemias of both B and T cell origin.[11] Early attempts with radiation therapy to treat A-T patients with cancer revealed another characteristic of the disease: profound clinical radiosensitivity.[12]

MR spectroscopy has been used to examine metabolite changes within autosomal recessive ataxias. This study sought to characterize the MR imaging appearances of A-T in adults, including the deposition of telangiectasia, by using MR spectroscopy to test the hypothesis that cerebellar metabolism in A-T patients would be abnormal relative to healthy controls.

Received January 12, 2006; accepted after revision March 7.

From the Academic Unit of Radiology, The University of Sheffield, Sheffield, United Kingdom (L.I.W., P.D.G., G.D., I.D.W.); The Department of Medical Genetics, Nottingham City Hospital, Nottingham, United Kingdom (S.J.R.); and the Department of Radiology, Royal Hallamshire Hospital, Sheffield, United Kingdom (C.A.J.R.).

Abstracts previously presented at: Annual Meeting of the British Chapter ISMRM, September 2005, Oxford, UK; British Society of Neuroradiologists Annual Scientific Meeting, October 2005, Cambridge, UK.

The work was supported by a grant from the Ataxia-Telangiectasia Society UK.

Address correspondence to Lauren I. Wallis, PhD, Academic Unit of Radiology, C Floor, Royal Hallamshire Hospital, Glossop Rd, Sheffield, South Yorkshire, S10 2JF England; e-mail: l.wallis@sheffield.ac.uk

Methods

Patients and Control Subjects

This study was approved by the South Sheffield Research Ethics Committee (University of Sheffield, Sheffield, United Kingdom) and was conducted in accordance with the declaration of Helsinki. Informed, written consent was obtained from all participants. The study group comprised 12 patients with known A-T (7 men, 5 women; mean age of 31.8 years, range of 23–47 years), recruited with the help of the Ataxia-Telangiectasia Society of the United Kingdom, and 12 healthy controls (6 men, 6 women; mean age of 33.0 years, range of 25–49 years). A *t* test comparing the ages of the A-T patients and controls revealed no significant age difference between groups ($t = -0.39$, $P = .70$).

MR Imaging Protocol

All subjects underwent MR investigation in a clinical system operating at 3T (Intera 3T, Philips Medical Systems, Best, Netherlands) in an 8-channel receive-only head coil. Immobilization aids were used to reduce the incidence of motion artifacts. Patients were positioned as symmetrically as possible within the head coil, and fine-tuning adjustments to section position were then made after the localizing scans were performed. The MR imaging protocol comprised axial T2-weighted turbo spin-echo imaging (TR = 3000 ms, TE = 80 ms, section thickness = 4 mm, section gap = 0 mm, field of view = 230 mm, 256 × 256 matrix reconstructed to 512 × 512), axial T2*-weighted images acquired by using a fast-field echo technique (TR = 1144 ms, TE = 18 ms, $\alpha = 18°$, section thickness = 4 mm, section gap = 0 mm, field of view = 230 mm, 256 × 512 matrix), and the acquisition of a high-resolution T1-weighted dataset via an magnetization-prepared rapid acquisition of gradient-echo technique (TR = 8300 ms, TE = 4.1 ms, $\alpha = 8°$, section thickness = 1 mm, field of view = 230 mm, 256 × 512 matrix). The axial sections for the T2- and T2*-weighted images were aligned on the anterior commissure–pos-

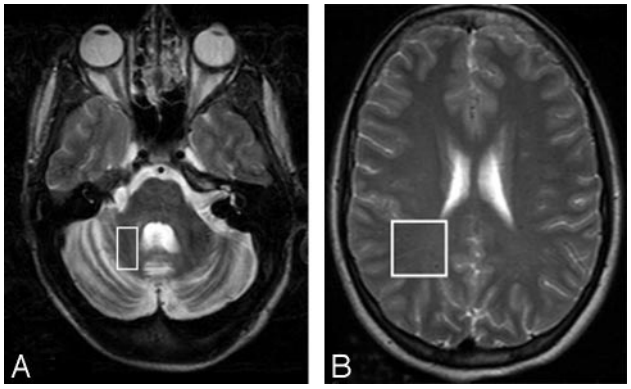

Fig 1. T2-weighted turbo spin-echo images from an A-T patient revealing severe atrophy of the cerebellar hemispheres with voxel placed in the region of the dentate nucleus (*A*) and with voxel placed in the parieto-occipital white matter (*B*).

terior commissure line, and the section positions were copied between the series of images to permit direct comparison of detection of any abnormalities. A qualitative evaluation of cerebellar atrophy (normal, mild, moderate, severe) was made by an experienced neuroradiologist (C.A.J.R.), who was blinded to the status of each subject. Telangiectasias were rated by using standard descriptions of "multiple hypointense foci on T2-weighted and gradient refocused imaging."[13]

Proton spectra were acquired with a point-resolved spectroscopy sequence technique (TR = 2000 ms, TE = 144 ms, 256 averages, 2048 data points, bandwidth = 4000 Hz) from 1) a 2 × 1 x 1-cm single voxel placed in the right cerebellar white matter, encompassing the dentate nucleus (Fig 1*A*); and 2) a 2 × 2 x 2-cm single voxel placed in the right peritrigonal parietooccipital white matter (Fig 1*B*). Both voxels were positioned to avoid inclusion of CSF within the volume of interest.

Spectra were analyzed by using the AMARES technique implemented in a third-party software package (MRUI) (software download available at http://www.mrui.uab.es/mrui/mrui_Overview.shtml).[14,15] After referencing to the *N*-acetylaspartate (NAA) peak (set to 2.02 ppm), data processing involved the following steps: filtered suppression of the water peak; zero filling; truncation; apodization of the corrected time-domain signal intensity by multiplying a Gaussian line broadening of 5 Hz, then by Lorentzian broadening of −5Hz; baseline correction followed by zero-order and first-order phase correction. Results are expressed as the ratios of the areas under the 3 prominent resonances due to NAA at 2.02 ppm, creatine (Cr) at 3.0 ppm, and choline (Cho) at 3.2 ppm.

Because of group sizes of 9, statistical analysis was performed with the nonparametric Mann-Whitney *U* test to compare for patient and control differences in the 3 ratios for each of the 2 voxel regions. This analysis resulted in 6 comparisons, and a Bonferroni correction defined the level of significance as $P = .0083$ (0.05/6).

Results

All 12 A-T patients were classified as having severe cerebellar atrophy (Figs 1*A*, 2*A*). Three of the controls were rated as having mild cerebellar atrophy; the remaining 9 were classified as normal. Four A-T patients had capillary telangiectasia (2 solitary, 2 multiple) best depicted on T2*-weighted imaging (Fig 3). Most of the telangiectasias were barely visible on the turbo spin-echo T2-weighted images, though some larger clusters were revealed as areas of hyperintensity. One person

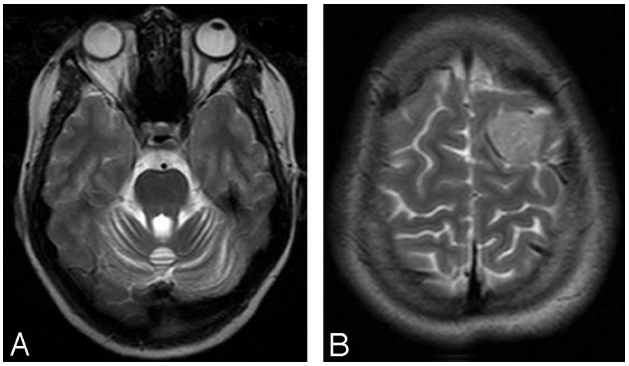

Fig 2. T2-weighted turbo spin-echo images from an A-T patient revealing severe atrophy of cerebellar vermis (*A*) and, in another patient, suspected meningioma (*B*).

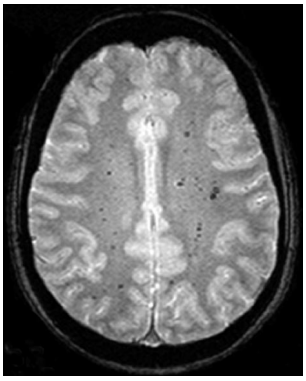

Fig 3. Representative T2*-weighted image from a 28-year-old A-T patient showing multiple capillary telangiectasia. Note the multiple punctate regions of hypointensity throughout the cortical white matter.

with A-T had an unexpected extra-axial mass overlying the left frontal lobe. This mass is under further investigation but most likely represents a meningioma (Fig 2*B*).

Spectra from 3 A-T patients were unusable due to poor quality spectra. Therefore, 9 controls were age-matched to the remaining patients for statistical analysis. Figure 4 shows sample spectra from an A-T patient and control for the parieto-occipital white matter and cerebellum regions.

Analysis for the cerebellar region (Fig 5) revealed significantly lower NAA/Cho ($P = .002$) and higher Cho/Cr ($P = .008$) in the A-T patients compared with controls. There was no significant group difference for the NAA/Cr ratio ($P = .796$). No significant group differences were found in any of the spectroscopic ratios from the parieto-occipital white matter region ($P > .5$) (Fig 6).

Discussion

The most pronounced neuropathologic changes in A-T occurred in the cerebellum, comprising atrophy of the hemispheres, vermis, and in some cases the dentate nucleus. This reflects pronounced loss of Purkinje and granule cells from the cerebellar cortex.[5,16] The presence of basket cells indicates that Purkinje cells are present initially but deteriorate during the course of the disease.[17]

Imaging studies of patients with A-T have supported these pathologic findings. A CT study of 5 patients showed cerebellar atrophy in 4 patients and discrete calcification of the lentiform nucleus in one patient.[18] A further CT study of 12 A-T

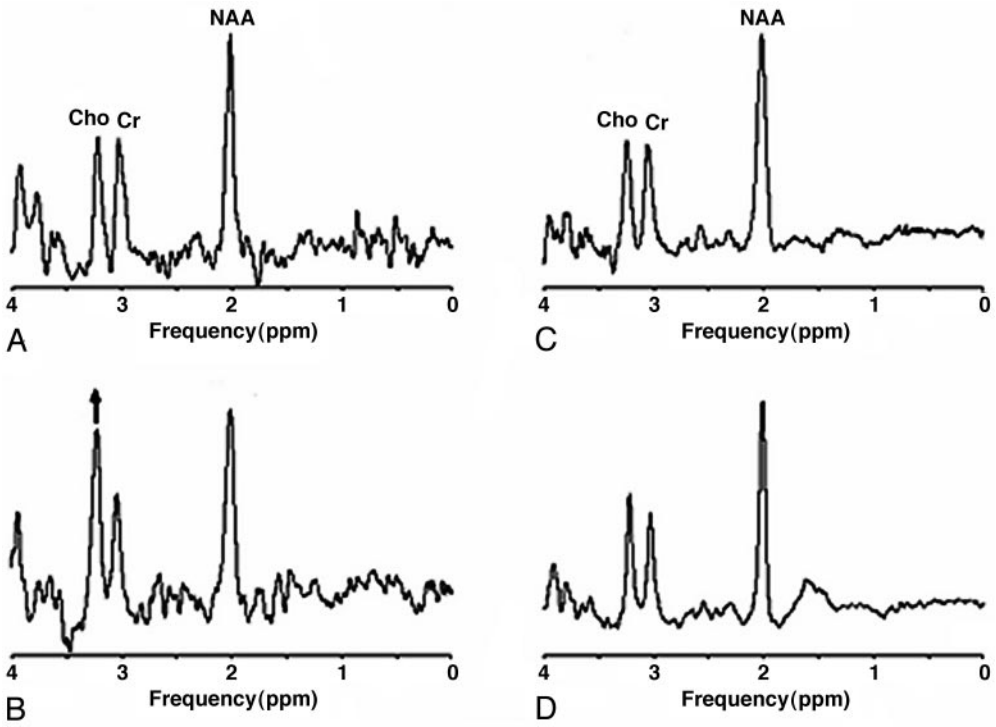

Fig 4. Proton MR spectra from the region of the dentate nucleus of a control subject (*A*) and a patient with A-T (*B*) and from the parieto-occipital white matter of a control subject (*C*) and a patient with A-T (*D*). The major metabolite peaks are labeled and correspond to cholines (Cho) at 3.2 ppm, creatines (Cr) at 3.0 ppm, and *N*-acetylaspartate (NAA) at 2.02 ppm. The increase in the Cho peak is marked with an arrow.

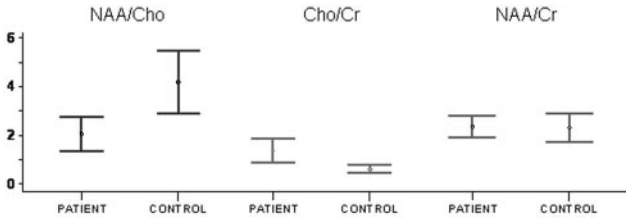

Fig 5. Plot of long echo-time ratios of *N*-acetylaspartate/choline (NAA/Cho) ($P = .002$), choline/creatine (Cho/Cr) ($P = .008$), and *N*-acetylaspartate/creatine (NAA/Cr) ($P = .796$) from voxels placed in the region of the dentate nucleus. Error bars indicate 95% CI from the mean.

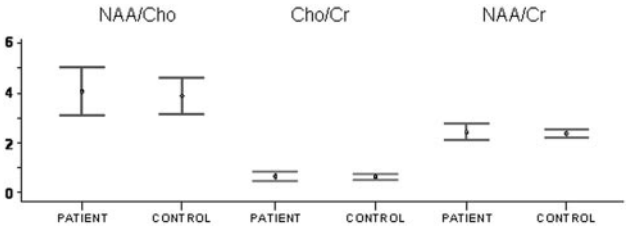

Fig 6. Plot of long echo-time ratios of *N*-acetylaspartate/choline (NAA/Cho) ($P = .546$), choline/creatine (Cho/Cr) ($P = .931$), and *N*-acetylaspartate/creatine (NAA/Cr) ($P = .796$) from voxels placed in the region of the parieto-occipital white matter. Error bars indicate 95% CI from the mean.

patients also revealed cerebellar atrophy, particularly of the vermis, and decreased thickness of the superior cortex of the cerebellar hemispheres in 5 of 11 patients. Other frequent signs included hypoplasia of the inferior vermis and a large cisterna magna.[19]

An MR imaging study of 5 male A-T patients aged between 9 and 28 years revealed vermian atrophy in 5 patients, with hemispheric atrophy present in 4 of the 5 patients.[20] A further MR imaging study of 19 patients aged 2 to 38 years reported most frequent involvement of the lateral hemispheres with subsequent progression to the superior and inferior portions until diffuse. The authors concluded that A-T begins with selective atrophy and that the severity is linked to duration of the disease.[21] All of the patients in our study were rated as having marked atrophy of both the cerebellar vermis and hemispheres. These patients were adults aged between 23 to 49 years, which may be reflective of the nonspecific anatomic location of their atrophies.

The detection of capillary telangiectasias is best seen on postcontrast T1-weighted images or, where contrast cannot be used, on T2*-weighted gradient-echo images.[22,23] Our finding of multiple brain telangiectasias in 2 patients (who were both noted to have ocular telangiectasia) and single telangiectasia in a further 2 patients concurs with reported cases of cerebral and brain stem telangiectasias.[24,25] The telangiectasias were best depicted on the T2*-weighted gradient-echo images.

The spectra were acquired with a long echo-time (TE = 144 m) technique and hence were T2-weighted. Changes in the relative metabolite resonance, or signal intensity, may be due to alterations in the metabolite's T2 relaxation time, concentration, or both.[26] Changes to the chemical environment of a metabolite will accordingly cause changes in T2 relaxation and may affect the signal intensity. The results obtained for the parieto-occipital white matter region did not differ between patients and controls. In contrast, the cerebellar metabolic pattern revealed significantly increased Cho/Cr and reduced NAA/Cho in the A-T patients, implying an increase in the choline signal intensity, with NAA/Cr showing no significant difference from that of the controls.

A recent review of the MR imaging and MR spectroscopy

findings for more than 60 different types of ataxias revealed the most common spectroscopic pattern in the cerebellar hemispheres and vermis to be reduced NAA; for example, moderate reductions in the absolute concentration of NAA in Friedrich ataxia, small decreases in spinocerebellar ataxia types 1 and 3, and severe decreases in spinocerebellar ataxia type 2.[27] A reduced NAA/Cr ratio has been reported in patients with spinocerebellar ataxia types 1 and 2.[28] Significant differences in mean NAA and NAA/Cho ratios have also been shown between patients with gluten-sensitive ataxia and controls.[29] In addition to changes in NAA, reductions in Cho/Cr have been shown in olivopontocerebellar ataxia and small reductions in absolute concentrations of choline in spinocerebellar ataxias 2 and 3.[27,30]

NAA is considered to be a neuronal marker, and reductions in the absolute concentration of NAA or in the NAA/Cr or NAA/Cho ratios reflect neuronal loss or damage.[31,32] The reductions in NAA seen in ataxia are generally considered to reflect the loss of neurons due to atrophic processes.[30] Our results suggest no decrease in the NAA signal intensity relative to the controls, despite visible cerebellar atrophy in all of the A-T patients. A decrease in NAA and Cr, with unaltered Cho, could also account for our ratio results, but a decrease in Cr is unlikely, as it remains fairly stable, even in disease.[31] It is possible that the NAA signal intensity is reduced, but that changes in the chemical environment due to atrophy have affected the T2, increasing the signal intensity per millimole and compensating for any reduction in absolute concentration.[26] Alternatively, the position of the voxel in the region of the dentate nucleus could be responsible for the lack of change in the NAA signal intensity. Neuropathologic studies of the A-T cerebellum have shown that while atrophy may be severe in the vermis and hemispheres, the dentate nucleus may remain intact or may develop atrophy at a later stage in the disease.[8,33]

An increase in the Cho signal intensity is not a typical finding in ataxia. The Cho resonance predominantly consists of phosphocholine and glycerophosphocholine, compounds involved in membrane synthesis and degradation, and therefore any inferred increase in the Cho resonance can indicate cellular proliferation or demyelination.[34,35] A study has shown increased Cho/Cr at long echo times but no change in Cho at short echo times in gluten ataxia, leading the authors to conclude that the T2 of the Cho signal intensity may have been affected by a change in chemical environment.[29] Our results do not give absolute concentrations for the metabolites, and it is possible that the raised Cho/Cr, obtained at long echo times, reflects such a process.

However, there are neuropathologic processes within A-T that may lead to changes in the Cho signal intensity. Demyelination has been reported in the medial lemniscus, the superior and inferior cerebellar peduncles, and the fasciculus gracilis but not within the cerebellar hemispheres, vermis, or dentate nucleus.[8,36] The postmortem finding of a few neurons in the early stages of degeneration has led to the suggestion that the atrophy in A-T is a continuous process of Purkinje cell death.[37] Therefore, the increase in Cho signal intensity may be indicative of active membrane breakdown, suggesting that their atrophy is an ongoing process. Alternatively, the increase may be due to gliosis, where an increase in the number of neuroglia and therefore in the overall number of cells would cause a high Cho signal intensity.[38,39] Use of short echo-time spectroscopy to measure myo-inositol, a glia cell marker, could confirm this.

Gliosis in A-T has been reported postmortem in the Purkinje, molecular, and granule cell layers and within the dentate nucleus.[8,33,36,37] Reactive astrocytes and activated microglia distributed throughout the cerebellum may suggest an immune response to the cerebellar neurodegeneration.[16] Astrocytes are particularly rich in Cho, and thus an increase in Cho may suggest astrocyte proliferation.[40] Astrocytes maintain high cellular concentrations of certain antioxidants and contribute to the antioxidant defense of neurons.[41,42] Gliosis seen in A-T could be due to an increased need for oxidative protection in the absence of normally functioning DNA repair mechanisms. Human A-T cells have been shown to be in a state of constant oxidative stress, with attendant chronic activation of stress response pathways in the cerebellum but not in the cerebrum.[43,44]

A-T is a rare condition, and though the results obtained were from a small group, they provide information about cerebellar metabolism in adult patients with established symptoms that appear to separate A-T from other ataxias. To assist in the diagnosis of A-T the next step would be to study patients in the early stages of neurodegeneration to see if spectroscopy can provide additive information about cerebellar functioning. If the pattern of raised Cho is found in early A-T, this may assist to in the differential diagnosis of A-T from other forms of ataxia. Differences in the spectroscopic findings for young and established patients may also help monitor treatments for A-T, as has been seen in gluten ataxia.[29]

Conclusions

This study examined a group of adult patients with A-T, showing marked cerebellar atrophy of the vermis and hemispheres in all. T2*-weighted gradient-echo imaging revealed multiple telangiectasias in 2 of the patients and single telangiectasia in one. MR spectroscopy of the cerebellum suggested an increase in the Cho signal intensity in A-T, but in contrast with other ataxias, no change in the NAA signal intensity was shown, suggesting a difference in the A-T cerebellar neuropathology. Further work is needed to assess cerebellar spectroscopy as a method for aiding early diagnosis of A-T.

Acknowledgments

The authors acknowledge the radiographers of the Academic Unit of Radiology based at the Royal Hallamshire Hospital (Sheffield, United Kingdom), Dr. M. Clemence of Philips Medical Systems for his spectroscopic input, and the sponsorship of the Ataxia-Telangiectasia Society of the United Kingdom.

References

1. Gatti RA, Berkel I, Boder E, et al. **Localization of an ataxia-telangiectasia gene to chromosome 11q22–23.** *Nature* 1998;336:577–78
2. Lange E, Borresen AL, Chen X, et al. **Localization of an ataxia-telangiectasia gene to an approximately 500-kb interval on chromosome 11q23.1: linkage analysis of 176 families by an international consortium.** *Am J Hum Genet* 1995;57:112–19
3. Savitsky K, Bar-Shira A, Gilad S, et al**. A single ataxia telangiectasia gene with a product similar to PI-3 kinase.** *Science* 1995;268:1749–53
4. Olsen JH, Hahnemann JM, Børresen-Dale A-L, et al. **Cancer in patients with**

ataxia-telangiectasia and in their relatives in the Nordic countries. *J Natl Cancer Inst* 2001;93:121–27
5. Jabado N, Concannon P, Gatti RA. **Ataxia-telangiectasia, a neurodegenerative disorder.** In: T Klockgether, ed. *Handbook of Ataxia Disorders.* New York: Marcel Dekker; 2000:163–90
6. Lederman HM, Crawford TO (2002) **Handbook for families and caregivers.** In: *A-T Children's Project* [online]. Available at: http://www.atcp.org/Handbook%20TOC.htm. Accessed January 2006
7. Farr AK, Shalev B, Crawford TO, et al. **Ocular manifestations of ataxia-telangiectasia.** *Am J Ophthalmol* 2002;134:891–95
8. Solitaire GB. **Louis-Bar's syndrome (ataxia-telangiectasia).** *Neurology* 1968;18:1180–86
9. Nowak-Wegryzn A, Crawford TO, Winkelstein JA, et al. **Immunodeficiency and infections in ataxia-telangiectasia.** *J Pediatr* 2003;144:505–11
10. Woods CG, Taylor AM. **Ataxia telangiectasia in the British Isles: the clinical and laboratory features of 70 affected individuals.** *Q J Med* 1992;82:169–79
11. Taylor AM, Metcalfe JA, Thick J, et al. **Leukemia and lymphoma in ataxia telangiectasia.** *Blood* 1996;87:423–38
12. Shiloh Y. **Ataxia telangiectasia and the Nijmegen breakage syndrome: related disorders but genes apart.** *Annu Rev Genet* 1997;31:635–62
13. Osborne AG, ed. *Diagnostic Neuroradiology.* St. Louis: Mosby-Year Book; 1994:309–11
14. Vanhamme L, van den Boogaart A, van Huffel S. **Improved methods for accurate and efficient quantification of MRS data with use of prior knowledge.** *J Magn Reson* 1997;129:35–43
15. de Beer R, van Ormondt D. **Analysis of NMR data using time domain fitting procedures.** In: Rudin M, ed. *NMR Basic Principles and Progress*. Vol 26. Berlin: Springer-Verlag; 1992:201–48
16. Perlman S, Becker-Catalina S, Gatti R. **Ataxia-telangiectasia: diagnosis and treatment.** *Semin Pediatr Neurol* 2003;10:173–82
17. Gatti RA, Vinters HV. **Cerebellar pathology in ataxia-telangiectasia: the significance of basket cells.** *Kroc Found Ser* 1985;19:225–32
18. Demaerel PH, Kendall BE, Kingsley D. **Cranial CT and MRI in diseases with DNA repair defects.** *Neuroradiology* 1992;34:117–21
19. Farina L, Uggetti C, Ottolini A, et al. **Ataxia-telangiectasia: MR and CT findings.** *J Comput Assist Tomogr* 1994;18:724–27
20. Sardanelli F, Parodi RC, Ottonello C, et al. **Cranial MRI in ataxia-telangiectasia.** *Neuroradiology* 1995;37:77–82
21. Tavani F, Zimmerman RA, Berry GT, et al. **Ataxia-telangiectasia: the pattern of cerebellar atrophy on MRI.** *Neuroradiology* 2003;45:315–19
22. Barr RM, Dillon WP, Wilson CB. **Slow-flow vascular malformations of the pons: capillary telangiectasias?** *AJNR Am J Neuroradiol* 1996;17:71–78
23. Lee RR, Becher MW, Benson ML, et al. **Brain capillary telangiectasia: MR imaging appearance and clinicohistopathologic findings.** *Neuroradiology* 1997;205:797–805
24. Ciemins JJ, Horowitz AL. **Abnormal white matter signal in ataxia-telangiectasia.** *AJNR Am J Neuroradiol* 2000;21:1483–85
25. Huddle DC, Chaloupka JC, Sehgal V. **Clinically aggressive diffuse capillary telangiectasia of the brain stem: a clinical radiologic-pathologic case study.** *AJNR Am J Neuroradiol* 1999;20:1674–77
26. Wilkinson ID, Paley M, Chong WK, et al. **Proton spectroscopy in HIV infection: relaxation times of cerebral metabolites.** *Magn Res Imag* 1994;12:951–57
27. Viau M, Boulanger Y. **Characterization of ataxias with magnetic resonance imaging and spectroscopy.** *Parkinsonism Relat Disord* 2004;10:335–51
28. Guerrini L, Lolli F, Ginestroni A, et al. **Brainstem degeneration correlates with clinical dysfunction in SCA1 but not SCA2. A qualitative volumetric, diffusion and proton spectroscopic MR study.** *Brain* 2004;127:1785–95
29. Wilkinson ID, Hadjivassiliou M, Dickson JM, et al. **Cerebellar abnormalities on proton MR spectroscopy in gluten ataxia.** *J Neurol Neurosurg Psychiatry* 2005;76:1011–13
30. Mascalchi M, Cosottini M, Lolli F, et al. **Proton MR spectroscopy of the cerebellum and pons in patients with degenerative ataxia.** *Radiology* 2002;223:371–78
31. Castillo M, Kwock L, Mukherji SK. **Clinical applications of proton MR spectroscopy.** *AJNR Am J Neuroradiol* 1996;17:1–15
32. Ross B, Bluml S. **Magnetic resonance spectroscopy of the human brain.** *Anat Rec* 2001;265:54–84
33. Perry TL, Kish SJ, Hinton D, et al. **Neurochemical abnormalities in a patient with ataxia-telangiectasia.** *Neurology* 1984;34:187–91
34. Soher BJ, van Zijl PC, Duyn JH, et al. **Quantitative proton MR spectroscopic imaging of the human brain.** *Magn Res Med* 1996;35:356–63
35. Burtscher IM, Holtås S. **Proton MR spectroscopy in clinical routine.** *J Magn Res Imag* 2001;13:560–67
36. Larnaout A, Belal S, Ben Hamida C, et al. **Atypical ataxia telangiectasias with early childhood lower motor neuron degeneration: a clinicopathological observation in three siblings.** *J Neurol* 1998;245:231–35
37. Paula-Barbosa MM, Ruela C, Tavares MA, et al. **Cerebellar cortex ultrastructure in ataxia-telangiectasia.** *Ann Neurol* 1983;13:297–302
38. Gill SS, Small RK, Thomas DG, et al. **Brain metabolites as 1H NMR markers of neuronal and glial disorders.** *NMR Biomed* 1989;2:196–200
39. Lai PH, Chen PC, Chang MH, et al. **In vivo proton MR spectroscopy of choreaballismus in diabetes mellitus.** *Neuroradiology* 2001;43:525–31
40. Scarabino T, Popolizio T, Bertolino A, et al. **Proton magnetic resonance spectroscopy of the brain in pediatric patients.** *Eur J Radiol* 1999;30:142–53
41. Wilson JX. **Antioxidant defense of the brain: a role for astrocytes.** *Can J Physiol Pharmacol* 1997;75:1149–63
42. Iida T, Furuta A, Nakabeppu Y, et al. **Defense mechanism to oxidative DNA damage in glial cells.** *Neuropathology* 2004;24:125–30
43. Rotman G, Shiloh Y. **ATM: from gene to function.** *Hum Mol Genet* 1998;7:1555–63
44. Watters DJ. **Oxidative stress in ataxia-telangiectasia.** *Redox Rep* 2002;8:23–29